Bioelectrochemistry and Biosensors
https://www.sciltp.com/journals/bebs

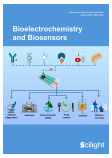

Article

Synergistic Bioinorganic Interfaces: Laccase-Like Nanozymes Coupled with Natural Laccase as Stable and High-Performance Cathodic Catalysts in Enzymatic Biofuel Cells

Olha Demkiv [1,2,*], Nataliya Stasyuk [1,2], Oksana Zakalska [1], Halyna Klepach [3], Galina Gayda [1] and Mykhailo Gonchar [1,3,*]

[1] Institute of Cell Biology, National Academy of Sciences of Ukraine, 79005 Lviv, Ukraine
[2] Institute of Physical Chemistry, Polish Academy of Sciences, 01-224 Warsaw, Poland
[3] Department of Biology and Chemistry, Drohobych Ivan Franko State Pedagogical University, 82100 Drohobych, Ukraine
* Correspondence: demkiv@yahoo.com (O.D.); mykhailo1952@gmail.com (M.G.)

How To Cite: Demkiv, O.; Stasyuk, N.; Zakalska, O.; et al. Synergistic Bioinorganic Interfaces: Laccase-like Nanozymes Coupled with Natural Laccase as Stable and High-Performance Cathodic Catalysts in Enzymatic Biofuel Cells. *Bioelectrochemistry and Biosensors* **2025**, *1*(1), 3

Received: 4 November 2025
Revised: 18 November 2025
Accepted: 24 November 2025
Published: 5 December 2025

Abstract: The limited kinetics of the oxygen reduction reaction (ORR) at the cathode remains a key bottleneck in improving the power output of enzymatic biofuel cells (EBFCs). In this study, we present a bioinorganic hybridization that integrates natural laccase (Lac) with laccase-like nanozymes (LacNZs) based on multimetallic composites to improve charge-transfer efficiency. The designed LacNZs structurally and functionally emulate the multicopper catalytic core of laccase, enabling accelerated electron transport and efficient ORR through a synergistic bioinorganic electron-transfer mechanism. EBFCs were fabricated by coupling an AOx/CNT-based bioanode with the constructed enzyme- and nanozyme-based cathodes containing either Lac, LacNZ, or laccase composites Lac/LacNZ, and all systems were evaluated under identical conditions. Incorporation of LacNZs into the cathodic layer resulted in a substantial enhancement of electrocatalytic activity and overall cell performance. The nCuCeAuZIF/Lac/GCE and nCoCuCeZIF/Lac/GCE hybrid cathodes demonstrated power densities of 3.4 $\mu W \cdot cm^{-2}$, OCV = 0.610 V, and 2.2 $\mu W \cdot cm^{-2}$, OCV = 0.550 V, respectively—nearly one order of magnitude higher than that of the enzyme Lac/CNT/GCE electrode. This improvement arises from the synergistic redox interplay among the multimetallic centers (Co, Cu, Ce, and Au) within the LacNZs, which effectively reproduce the T1–T3 copper sites of native laccase, thereby facilitating a direct four-electron reduction of O_2 to H_2O, enhancing electron mobility, and stabilizing the enzyme's conformation at the bioinorganic interface. The hybrid cathode also exhibited outstanding stability: retaining 75% of initial activity after 10 days (vs. 30% for Lac/GCE) and showing a 7.5% increase in sensitivity under 0.25 M NaCl (vs. 41.7% loss for Lac/GCE). Notably, EBFCs with only-LacNZs-based cathodes (nCuCeAu/GCE and nCoCuCeZIF/GCE) retained significant ORR activity (up to 1.2 $\mu W \cdot cm^{-2}$ and 0.53 $\mu W \cdot cm^{-2}$), highlighting their potential as enzyme-free, durable, and cost-effective catalysts. Nanozymes as catalytic elements of EBFCs can be regarded as an alternative to direct electron transfer technology, which is still complicated for proteins enzymes.

Keywords: enzymatic biofuel cells; laccase-like nanozyme; bioanode; biocathode; alcohol-oxidase; laccase

1. Introduction

The growing global demand for renewable and sustainable energy has stimulated intensive research into enzymatic biofuel cells (EBFCs) as environmentally benign power sources [1–3]. These systems employ biological or bioinspired catalysts to convert chemical energy from biofuels directly into electrical energy under mild conditions, typically at ambient temperature and neutral pH [4]. The overall performance of EBFCs is, however, critically limited by the oxygen reduction reaction (ORR) at the cathode, which remains, often the rate-determining step of the entire cell [3].

Traditionally, multicopper oxidases, primarily laccase and bilirubin oxidase, have served as cathodic catalysts due to their ability to mediate the four-electron reduction of molecular oxygen (O_2) to water (H_2O) without generating hydrogen peroxide (H_2O_2) intermediates [5]. Among these, fungal laccase from *Trametes versicolor, Trametes hirsuta*, and *Pleurotus ostreatus* are most widely employed owing to their high redox potential (E ≈ 0.78–0.79 V vs. NHE) and the presence of multiple copper centers (T1, T2, T3) that enable efficient intramolecular electron transfer [4–6]. Despite their excellent selectivity and bioelectrocatalytic efficiency, natural laccase exhibit several intrinsic drawbacks: a narrow pH tolerance (typically 3.5–5.0), limited thermal stability, and progressive deactivation under operational potentials [6]. For instance, a typical laccase-based cathode exhibits an onset potential around 0.6 V vs. Ag/AgCl and a current density of 0.4–0.6 $mA \cdot cm^{-2}$ under neutral conditions, which gradually decreases due to enzyme denaturation or copper center leaching.

Alternative oxidases such as bilirubin oxidase from *Myrothecium verrucaria* or *Magnaporthe oryzae* can operate closer to neutral pH (6.5–7.0) while maintaining ORR activity at ~0.55–0.65 V vs. Ag/AgCl [7]. However, the high production cost, limited availability, and sensitivity to inhibitors restrict their practical implementation. Similarly, tyrosinase, another copper-dependent oxidase, exhibits inferior turnover rates and pronounced substrate inhibition, making it less suitable for stable biocathodes.

To improve electron transfer efficiency between the redox sites of enzymes and the electrode surface, redox mediators such as ABTS, ferrocene derivatives, and osmium complexes have been employed to facilitate mediated electron transfer. While this strategy enhances current output, it also introduces additional kinetic losses and biocompatibility issues. On the other hand, immobilization of laccase on conductive nanostructures—such as carbon nanotubes (CNTs), graphene, or conductive polymers (PANI, PEDOT:PSS)—has improved electrode performance, but enzyme instability and reproducibility remain persistent challenges [1–3].

In recent years, nanomaterials and nanozymes (NZs) have emerged as a compelling alternative to natural enzymes. NZs are nanostructured materials capable of mimicking enzymatic catalysis, combining the redox selectivity of biological systems with the stability and conductivity of inorganic catalysts [8]. In the context of EBFCs, laccase (Lac), laccase-like nanozymes (LacNZs) have attracted particular attention for their ability to catalyze the ORR via multi-electron transfer pathways involving redox-active metal centers (Cu^{2+}/Cu^{+}, Fe^{3+}/Fe^{2+}, and Ce^{4+}/Ce^{3+}). These active sites reproduce the function of the trinuclear copper cluster in natural laccase, enabling efficient oxygen adsorption, activation, and reduction.

Various classes of nanomaterials have been reported to exhibit laccase-like oxidoreductase activity, including copper oxides (CuO, Cu_2O), spinel-type oxides ($NiCo_2O_4$, $CoFe_2O_4$), perovskites ($LaFeO_3$, $SrCoO_3$), and noble-metal composites (AuPt, CuPt, $AuCeO_2$) [8–13]. For example, CuO nanoparticles can catalyze ORR with an onset potential of 0.52 V vs. Ag/AgCl, whereas Au–CeO_2 composites achieve superior activity through Ce^{4+}/Ce^{3+} redox cycling that enhances oxygen vacancy formation and O_2 activation. Hybrid systems such as CuPt or AuCePt exhibit synergistic effects between the oxygen adsorption capacity of Pt and the redox dynamics of transition metals, leading to broader operational pH windows (3–9) and higher durability.

Unlike conventional metallic nanoparticles that act primarily as conductive enhancers [14], the ZIF-8–derived LacNZs represent a more high catalytic activity due to their highly porous and ordered structure, which enables controlled incorporation and spatial arrangement of multiple metal centers (Co, Cu, Ce, Au). This architecture provides catalytic activity that simulate natural laccase, yielding a different and more relevant mechanism natural laccase for promoting the four-electron ORR. Moreover, the ZIF-LacNZs facilitate more efficient synergistic electron transfer and markedly improve catalytic stability compared to the nanomaterial nCuPt and nAuCePt. These observations underscore the potential of LacNZs as either replacements or co-catalysts for natural enzymes in biocathodic applications. These observations underscore the potential of LacNZs as either replacements or co-catalysts for natural enzymes in biocathodic applications. Unlike nature laccase, NZs are resistant to denaturation, thermal stress, and chemical inhibitors, and can maintain activity under harsh electrochemical conditions. Their incorporation into hybrid architectures with biological catalysts enables synergistic redox coupling, enhancing both catalytic turnover and electron transfer efficiency.

Therefore, the rational design of hybrid cathodes (enzyme/NZs) that integrate natural laccase with laccase-mimetic nanoparticles holds great promise for achieving efficient, durable, and cost-effective ORR catalysis under physiological conditions. When immobilized onto conductive frameworks such as CNTs, these hybrids offer a large electroactive surface area, efficient charge transport, and improved long-term operational stability.

In this study, we developed a series of hybrid cathodes combining natural fungal laccase with various LacNZs (nCoZIF, nCuZIF, nPtCu, nCoCuCeZIF, and nCuCeAuZIF). Their electrocatalytic performance toward oxygen reduction was compared with that of electrodes modified with natural laccase alone and with LacNZs alone. The influence of NZ composition on the electrocatalytic activity, internal resistance, and durability of complete biofuel cells was analyzed. Our findings reveal that LacNZs not only can substitute natural laccase in ORR catalysis, but also synergistically enhance its activity when co-immobilized, resulting in up to an order-of-magnitude improvement in power density. This work establishes a fundamental framework for the design of next-generation hybrid cathodes, merging bioinspired catalysis with nanostructured redox materials for efficient and sustainable energy conversion.

2. Materials and Methods

2.1. Reagents and Materials

We used purified laccase (Lac) (EC 1.10.3.2) from *Trametes zonata*, and alcohol oxidase (AOx, EC 1.1.3.13) isolated from the yeast *Ogataea polymorpha*. Hydroquinone (HQ), and 2,2′-azino-bis(3-ethylbenzothiazoline-6-sulfonic acid) (ABTS) were purchased from Sigma-Aldrich (USA). Carbon nanotubes (CNTs, 95%) were obtained from Nanocyl (Sambreville, Belgium). Metal precursors (H_2PtCl_6, $Cu(NO_3)_2$, $Co(NO_3)_2$, $Ce(NO_3)_3$, and $HAuCl_4$ were of analytical grade. Phosphate buffer (PB, 50 mM, pH 7.0) or acetic buffer (AB, pH 4.5) served as the supporting electrolyte.

2.2. Synthesis of Laccase-Like Nanozymes

Five types of multimetallic LacNZs were synthesized: nCuZIF, nCoZIF, nCuPt, nCoCuCeZIF, and nCuCeAuZIF, following modified solvothermal or reduction methods. nCuZIF NPs were synthesized via a hydrothermal method using $Cu(NO_3)_2{\cdot}3H_2O$ and 2-methylimidazole as precursors. Solution A was prepared by dissolving 2.0 g 2-methylimidazole in 50 mL of methanol, while solution B contained 0.24 g $Cu(NO_3)_2{\cdot}3H_2O$ dissolved in 50 mL of methanol. Solution B was gradually added to solution A under constant stirring, producing a homogeneous blue suspension. The mixture was transferred into a autoclave and heated at 120 °C for 2 h. After cooling, the resulting solid was separated by centrifugation (9000 rpm, 10 min), washed three times with methanol, and dried at 70 °C overnight.

nCoZIF NPs were prepared at room-temperature. Solution A was prepared by dissolving 2.0 g 2-methylimidazole in 50 mL methanol. Solution B was obtained by dissolving 0.4 g $Cu(NO_3)_2{\cdot}6H_2O$ in 50 mL methanol. Under continuous stirring, solution B was slowly added to solution A, resulting in an immediate color change to violet, indicating the formation of ZIF-67. The mixture was further stirred for 5 h at room temperature. The obtained precipitate was separated by centrifugation (9000 rpm, 10 min), washed three times with methanol, and dried in an oven at 70 °C overnight.

nCuPt NPs were obtained through two sequential reduction steps. First, Pt NP were generated by adding $NaBH_4$ (10 mM) to a 5 mM H_2PtCl_6 solution in the presence of 10 mM sodium citrate at 60 °C under stirring for 15 min. Subsequently, an aqueous solution of $CuSO_4$ (10 mM) and PVP (0.1 wt%) was introduced, followed by reduction with ascorbic acid (3-fold molar excess). The mixture was heated at 90 °C for 45 min. The resulting nCuPt nanoparticles were separated by centrifugation and washed with deionized water.

nCoCuCeZIF NPs were synthesized via a modified one-pot solvothermal method. 0.01 M $Co(NO_3)_2{\cdot}6H_2O$, 0.01 M $Cu(NO_3)_2{\cdot}3H_2O$, and 0.01 M $Ce(NO_3)_3{\cdot}6H_2O$ were prepared in a deionized water under magnetic stirring. Subsequently, 2-methylimidazole (0.2 M, 10 mL) was added to form a ZIF-like NZs. The pH was adjusted to 9.5 by dropwise addition of 0.1 M NaOH to facilitate hydroxide precursor formation and stabilize metal–ligand complexes. The resulting suspension was transferred into autoclave and maintained at 120 °C for 2 h. After cooling, the precipitate was collected by centrifugation (9000 rpm, 10 min), washed three times with ethanol and deionized water, and dried at 70 °C overnight.

nCuCeAuZIF NPs were prepared through a two-step process. 0.01 M $Cu(NO_3)_2{\cdot}3H_2O$ and 0.005 M $Ce(NO_3)_3{\cdot}6H_2O$ were dissolved in 50 mL of deionized water. Subsequently, 2-methylimidazole (0.2 M, 10 mL) was added. The mixture was stirred at room temperature for 4 h until a light-blue precipitate appeared, indicating

the successful nucleation of CuCe–ZIF precursor. The obtained precipitate was collected by centrifugation (9000 rpm, 10 min), washed twice with deionized water and ethanol, and dried at 120 °C overnight.

2.3. Fabrication of the Enzymatic Fuel Cell

Bio- or hybrid electrodes were constructed using alcohol oxidase (AOx) (anode) and laccase (cathode) immobilized on glassy carbon electrodes (GCEs), either in their natural form (control) or combined with CNTs and LacNZs, following the general configuration enzyme/NPs/GCE.

For bioanode preparation, aliquots (3 μL) of AOx solution (50 $U \cdot mL^{-1}$, 50 mM PB, pH 7.5) were drop-cast onto CNT-modified GCEs, followed by drying at room temperature. CNTs were used exclusively for the anode configuration and were not employed for cathode fabrication. The AOx-based bioanode operated in 50 mM PB (pH 7.5) containing 0.5 mM ethanol as substrate and hydroquinone (HQ) as the redox mediator [14].

The cathodes were fabricated by depositing 2 μL laccase solution (10 $U \cdot mL^{-1}$, 50 mM AB, pH 4.5) either alone (Lac/GCE), or combined with LacNZs (Lac/nCuZIF/GCE, Lac/nCoZIF/GCE, Lac/nPtCu/GCE, Lac/nCoCuCeZIF/GCE and Lac/nCuCeAuZIF/GCE), as well as containing only LacNZs (nCuCeAuZIF/GCE, and nCoCuCeZIF/GCE). The modified electrode surfaces were coated with a thin 1% Nafion layer to enhance stability and prevent enzyme leaching. The three-type cathode functioned in 10 mL of 50 mM AB (pH 4.5) containing 1 mM ABTS.

The electrochemical performance parameters of the assembled EBFCs—including current density, power density, and open-circuit voltage (OCV)—were determined according to previously reported procedures All prepared electrodes were rinsed with the corresponding buffer solutions and stored at 4 °C until use.

2.4. Apparatus and Electrochemical Techniques

Morphological and compositional analyses of the prepared LacNZs and modified electrodes were performed using scanning electron microscopy (SEM) (FEI Nova NanoSEM 450) and X-ray photoelectron spectroscopy (XPS) (Microlab 350, Thermo Electron, East Grinstead, UK). Electrochemical measurements, including cyclic voltammetry (CV), and power density measurements**,** were performed at room temperature using an Autolab PGSTAT 302N (Metrohm, Barendrecht, The Netherlands).

All measurements were performed used a three-electrode mode, comprising a modified glassy carbon electrode (GCE) as the working electrode, a platinum wire as the counter electrode, and an Ag/AgCl (3 M KCl) electrode as the reference. The electrocatalytic performance of the enzymatic biofuel cells (EBFCs) was evaluated using polarization curves in a two-electrode configuration.

2.5. Statistical Analysis

All experiments were performed in triplicate (n = 3), and each measurement was conducted in duplicate to ensure reproducibility. Data are presented as mean ± standard deviation (SD). Statistical analysis and graphical plotting were carried out using OriginPro 8.5 (OriginLab Corporation, Northampton, MA, USA).

3. Results and Discussion

3.1. Laccase-Like Activity of Metal-Based Nanozymes

A series of single-component and hybrid metal-based nanostructures—nCuZIF, nCoZIF, nCuPt, nCoCuCeZIF, and nCuCeAuZIF—were synthesized using different approaches, including solvothermal precipitation of metal–organic frameworks (ZIFs) and two-step chemical reduction. The obtained nanomaterials were evaluated for their oxidoreductase activity (laccase-like) using (2,2′-azino-bis(3-ethylbenzothiazoline-6-sulfonic acid)) (ABTS) as a chromogenic substrate in 50 mM AB (pH 4.5).

Among the tested nanoparticles (NPs), the hybrid multimetallic-composites exhibited the highest activity in solution: nCoCuCeZIF, nCuPt, and nCuCeAuZIF showed specific activities of approximately 3.9, 3.4, and 3.5 $U \cdot mg^{-1}$, respectively (Figure 1). In contrast, the ZIF-based monometallic NZs, nCuZIF and nCoZIF, demonstrated lower activity values 2.5 U/mg and 2.3 U/mg, respectively. They correspond to roughly 2.6–4.4-fold lower compared with the native fungal laccase of *T. zonata*.

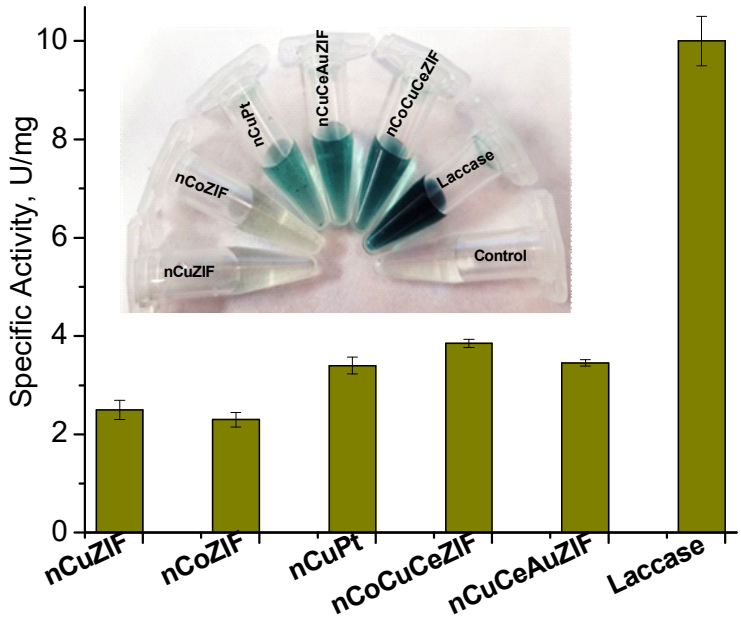

Figure 1. Comparative laccase-like activity of the metal-based NPs—nCuZIF, nCoZIF, nCuPtZIF, nCoCuCeZIF, and nCuCeAuZIF—in comparison with natural laccase *T. zonata*. Assays were performed in 50 mM AB (pH 4.5) using 1 mM ABTS as the substrate and a catalyst concentration of 1 mg·mL^{-1}.

Despite their comparatively lower catalytic activity, all LacNZs exhibited high storage stability. They maintained high catalytic efficiency over a broad pH range (3.0–7.5). Whereas the fungal laccase from *T. zonata* rapidly loses activity above pH 5.5 or at elevated temperatures, the LacNZs preserved more than 85% of their initial activity under the same conditions. Moreover, the NZs retained high catalytic performance even under high ionic strength (up to 250 mM NaCl), where the natural enzyme underwent a pronounced and irreversible loss of activity [14].

The exceptional robustness of the LacNZs—particularly nCuCeAuZIF and nCoCuCeZIF—underscores their potential as cost-effective, durable, and reusable alternatives to natural laccase. Their enhanced tolerance to environmental variations makes them highly promising candidates for biocatalytic, electrochemical, and environmental applications, including biosensing.

3.2. Structural and Morphological Characterization of the Nanozymes

The synthesized multimetallic LacNZs—nCoCuCeZIF, nCuCeAuZIF, and nCuPt—exhibited uniform nanoscale morphology and well-defined surface structures, as confirmed by Scanning Electron Microscopy (SEM) (Figure 2a,d,g) and Energy-Dispersive X-ray Spectroscopy (EDS) analysis (Figure 2c,f,i). SEM micrographs revealed morphology variations from porous sponge-like architectures to polyhedral nanoparticles (40–80 nm), depending on metal composition and synthetic route (Figure 2a,d,g). EDS data confirmed the successful incorporation and relative metal content of all selected elements Cu, Pt, Co, Ce, Au in synthesized NZs.

The nCoCuCeZIF NPs exhibited a porous, sponge-like architecture consisting of aggregates built from interconnected nanoscale crystallites (Figure 2d). This morphology is characteristic of mixed-metal oxides (Me_xO_y) generated from co-precipitated precursors. EDS analysis confirmed homogeneous distribution of Co, Cu, Ce, and O with mixed oxides (Co_xO_y, CeO_x). The presence of Ce-enriched regions suggests the generation of oxygen vacancies, which may enhance the redox flexibility and catalytic efficiency of this composite.

The nCuCeAuZIF hybrid NPs have structure prone to agglomeration, with quantitative EDS (Figure 2f) showing Au (~46.3 at%), Ce (~35.9 at%), and Cu (~7.5 at%), confirming successful formation a ternary composite. The high content of Au and Ce highlights their dominant structural and catalytic roles, where Au^0 facilitates electron delocalization, and Ce^{3+}/Ce^{4+} cycling promotes oxygen activation—both key features for mimicking the multicopper redox centers of natural laccase.

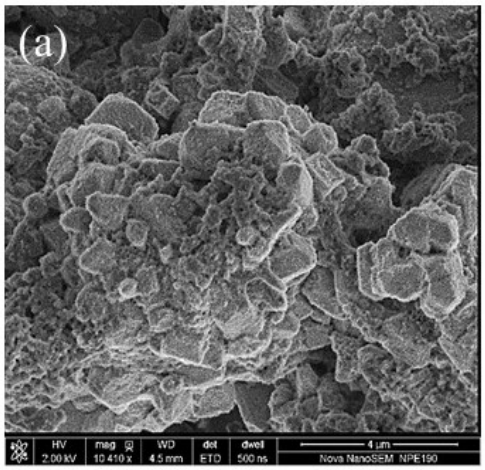

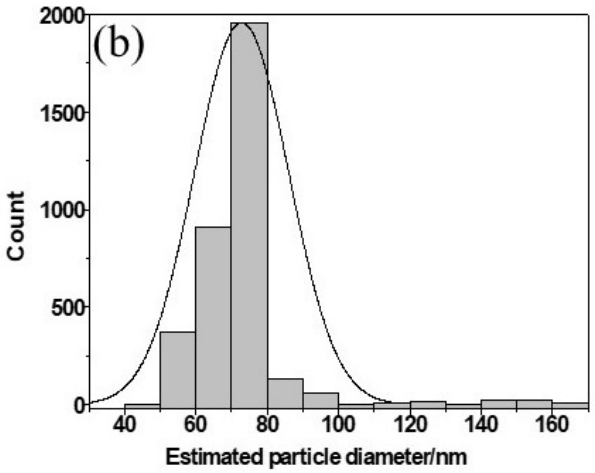

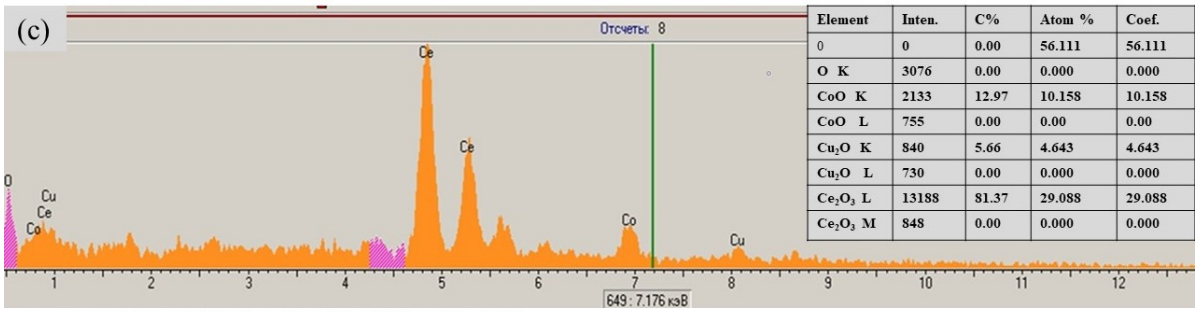

Element	Inten.	C%	Atom %	Coef.
0	0	0.00	56.111	56.111
O K	3076	0.00	0.000	0.000
CoO K	2133	12.97	10.158	10.158
CoO L	755	0.00	0.00	0.00
Cu_2O K	840	5.66	4.643	4.643
Cu_2O L	730	0.00	0.000	0.000
Ce_2O_3 L	13188	81.37	29.088	29.088
Ce_2O_3 M	848	0.00	0.000	0.000

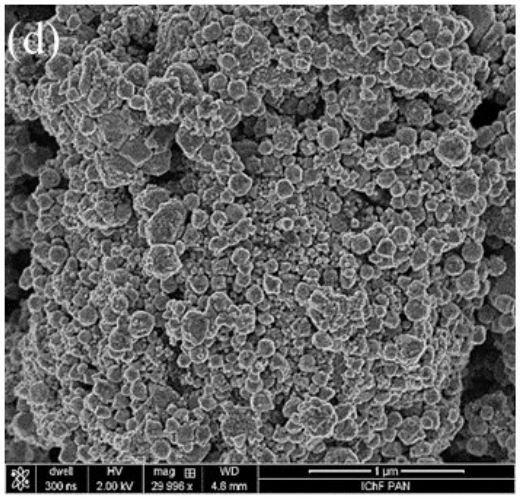

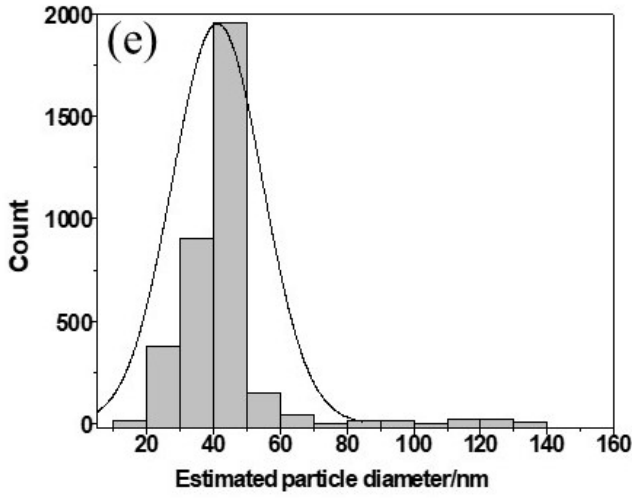

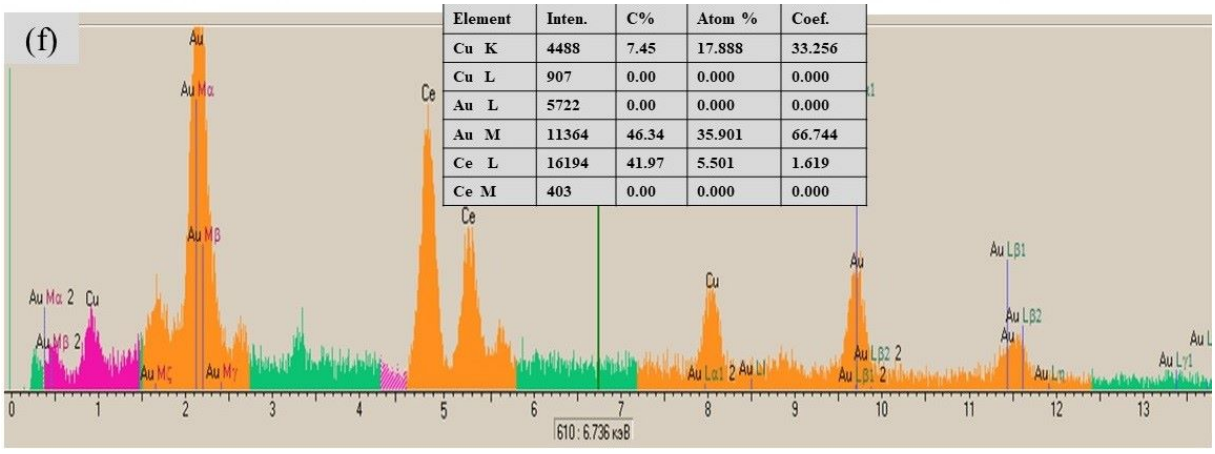

Element	Inten.	C%	Atom %	Coef.
Cu K	4488	7.45	17.888	33.256
Cu L	907	0.00	0.000	0.000
Au L	5722	0.00	0.000	0.000
Au M	11364	46.34	35.901	66.744
Ce L	16194	41.97	5.501	1.619
Ce M	403	0.00	0.000	0.000

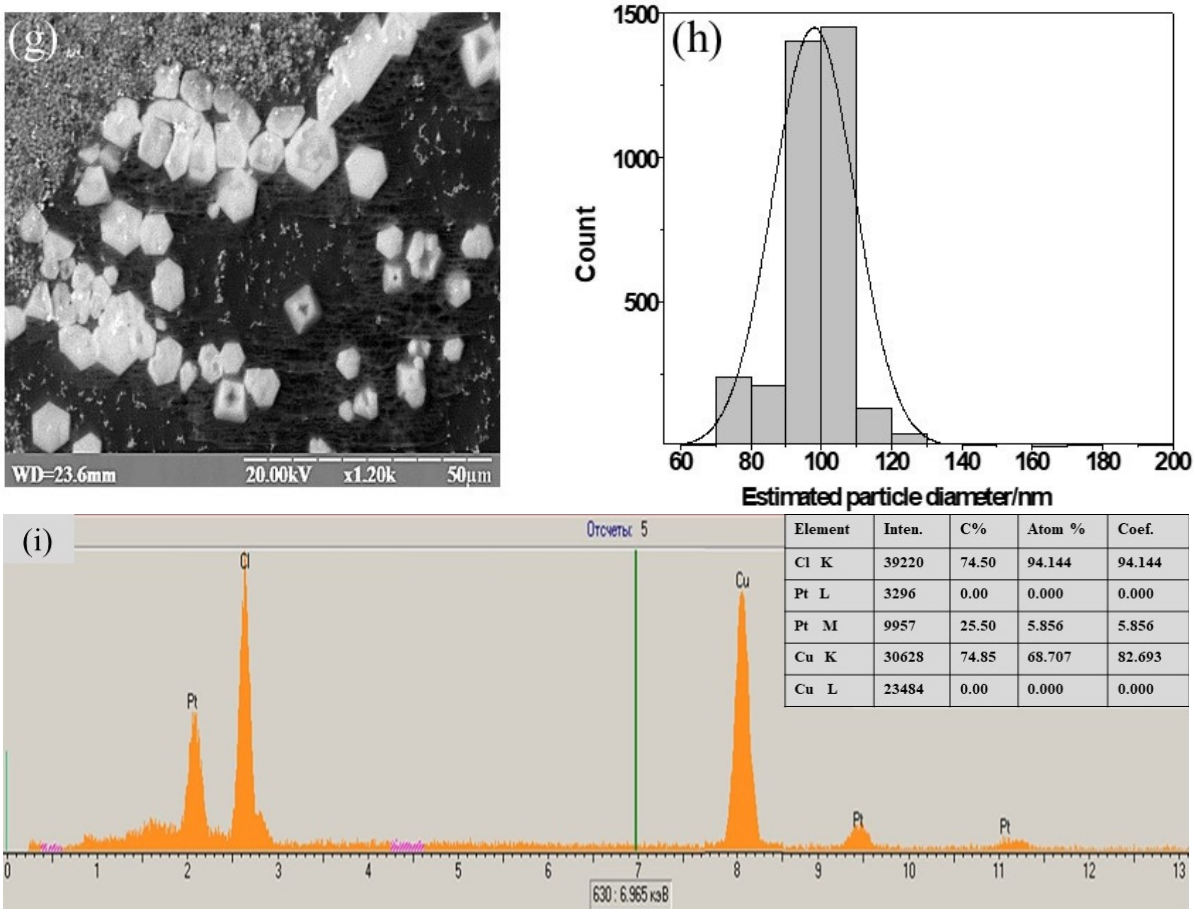

Element	Inten.	C%	Atom %	Coef.
Cl K	39220	74.50	94.144	94.144
Pt L	3296	0.00	0.000	0.000
Pt M	9957	25.50	5.856	5.856
Cu K	30628	74.85	68.707	82.693
Cu L	23484	0.00	0.000	0.000

Figure 2. Structural and elemental characterization of LacNZ: nCoCuCeZIF (**a**–**c**), nCuCeAuZIF (**d**–**f**), and nCuPt (**g**–**i**). (**a**,**d**,**g**) SEM images; (**b**,**e**,**h**) EDS spectra; and (**c**,**f**,**i**) particle size distribution.

The nCuPt NPs, prepared via sequential chemical reduction, displayed polyhedral morphologies (truncated cubic and octahedral) (Figure 2g). EDS (Figure 2i) confirmed Cu and Pt incorporation (Pt:Cu). Uniform elemental distribution supports bimetallic synergy, enabling effective electron transfer between Cu^{+}/Cu^{2+} and Pt^{0}/Pt^{2+} redox pairs.

EDS analysis of the LacNZs (nCoCuCeZIF, nCuCeAuZIF та nCuPt) (Figure 2 c,f,i) revealed the coexistence of multiple redox-active states across all three NZ compositions, including Cu^{+}/Cu^{2+} (932.4/934.7 eV), Co^{2+}/Co^{3+} (780.9/782.3 eV), Ce^{3+}/Ce^{4+} (882.0/885.4 eV), Pt^{0} (71.2 eV), and Au^{0} (83.8 eV). The presence several of these states confirms the formation of a multi-site electron-transfer network, functionally analogous to the T1–T3 copper clusters in natural laccase. The Ce^{3+}/Ce^{4+} redox couple enables oxygen-vacancy formation and reversible O_2 adsorption, whereas metallic Pt^{0} and Au^{0} contribute to enhanced electron mobility and structural stability. Together, these features create an integrated catalytic environment capable of promoting an efficient four-electron oxygen reduction reaction (ORR).

Therefore, the combination of structural heterogeneity, redox versatility, and metal–metal cooperation supports the proposed mechanism of bioinspired ORR catalysis in the developed LacNZs, making them promising platforms for electrocatalytic and biosensing applications.

3.3. Electrochemical Characterization of Cathodes Based on Laccase and Its Nanomimetics

The electrochemical behavior of the synthesized LacNZs—including nCuCeAuZIF, nCoCuCeZIF, and nCuPt—was investigated to elucidate their redox activity, oxygen reduction capability, and potential as efficient cathodic catalysts in biofuel cells. Cyclic voltammetry (CV) was employed to assess electron-transfer properties and catalytic performance. Figure 3 presents the CV profiles of the bare and modified LacNZs-based electrodes in 5 mM $K_3[Fe(CN)_6$ solution containing 0.1 M KCl at a scan rate of 50 mV/s and a step potential (E_{step}) of 2 mV.

All electrodes exhibited well-defined quasi-reversible redox peaks centered at approximately +0.30 V (anodic) and +0.20 V (cathodic) versus Ag/AgCl, corresponding to the $[Fe(CN)_6]^{3-/4-}$ redox couple and indicative of surface-confined electron-transfer processes involving multivalent metal centers. The introduction of LacNZs significantly increased peak currents compared to bare GCE and monometallic ZIF-based materials, in agreement with the quantitative values in Table 1. Three modified electrodes (nCuPt/GCE: +152/−121 μA; nCoCuCe/GCE:

+167/−140 μA; nCuCeAuZIF/GCE: +183/−152 μA) showed substantially enhanced electron-transfer kinetics and a larger electroactive surface area relative to both bare GCE (+140/−103 μA) and simple ZIF-based materials (nCoZIF and nCuZIF).

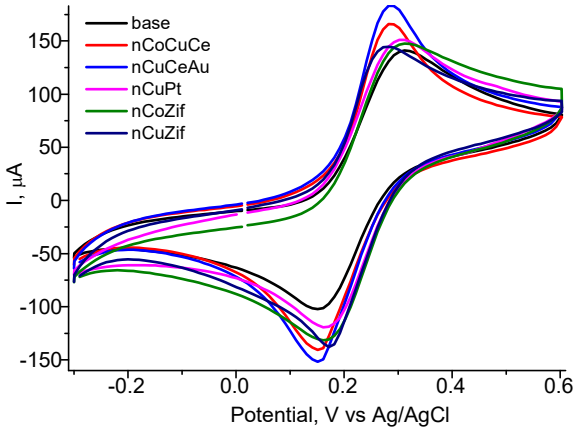

Figure 3. CV of bare and only-LacNZs-based electrodes (nCuZIF/GCE, nCoZIF/GCE, nCuPt/GCE, nCoCuCeZIF/GCE, and nCuCeAuZIF/GCE) in a 5 mM $K_3[Fe(CN)_6$ solution containing 0.1 M KCl at a scan rate of 50 mV/s, showing quasi-reversible redox peaks with anodic/cathodic currents increasing in the order GCE < nCoZIF < nCuZIF < nCuPt < nCoCuCeZIF < nCuCeAuZIF, reflecting enhanced electron-transfer and electroactive surface area.

Table 1. Electrochemical parameters of LacNZ-based electrodes (compared with bare electrode).

Electrode	Peak Current, Ox (μA)	Peak Current, Red (μA)	Epa (V)	Epc (V)	ΔEp (V)	Electroactive Surface Area (cm^2)
Bare (GCE)	+140	−103	+0.313	+0.153	0.160	0.169
nCoZIF/GCE	+148	−132	+0.310	+0.163	0.147	0.179
nCuZIF/GCE	+144	−137	+0.278	+0.172	0.106	0.174
nCuPt/GCE	+152	−121	+0.30	+0.168	0.132	0.183
nCoCuCeZIF/GCE	+167	−140	+0.288	+0.152	0.136	0.201
nCuCeAuZIF/GCE	+183	−152	+0.285	+0.152	0.133	0.221

Among the tested only-LacNZs-based electrodes, the nCuCeAuZIF-modified electrode exhibited the the highest peak currents (+183 μA/−152 μA), reflecting a higher of accessible redox sites and improved conductivity within. The electroactive surface area (A) was estimated using the Randles–Ševčík equation, assuming a diffusion coefficient of 7.6×10^{-6} $cm^2 \cdot s^{-1}$ for the $[Fe(CN)_6]^{3-}$ probe. The calculated area for nCuCeAuZIF (0.221 cm^2) greatly exceeded the geometric surface of the GCE (≈0.0707 cm^2), confirming substantial electroactive surface area enlargement and efficient charge transport facilitated by the LacNZ coating.

The separation between anodic and cathodic peaks (ΔE_p) provided further insight into charge-transfer behavior. While the bare electrode displayed ΔE_p 0.160 V, indicative of quasi-reversible kinetics, the nCuCeAuZIF/GCE showed ΔE_p 0.133 V, suggesting improved electron-transfer kinetics despite slight differences in peak potential due to nanostructuring. Despite this, the overall current response was markedly improved, reflecting the presence of multiple electroactive sites and enhanced catalytic turnover.

The tendency of anodic/cathodic peak currents followed the order: GCE < nCoZIF < nCuZIF < nCuPt < nCoCuCeZIF < nCuCeAuZIF, which is consistent with the increasing multimetallic composition and the measured electrochemical parameters (Table 1). Incorporation of LacNZs into the catalytic layer further increases these effects. Hybrid cathodes (Lac/LacNZ/GCE) displayed significantly enhanced redox peak currents compared with only the enzyme-based electrode (Lac/GCE), confirming accelerated electron transport at the bioinorganic interface. A distinct cathodic peak appeared at approximately 0.52 V (vs. Ag/AgCl), characteristic of the $O_2 \rightarrow H_2O$ reduction, validating the ORR catalytic activity of the hybrid electrodes.

The CV results clearly confirm that integration of LacNZs—particularly in the nCuCeAuZIF/Lac configuration—markedly enhances electron-transfer kinetics, increases electroactive surface area, and stabilizes redox processes at the electrode interface. These findings establish LacNZ-based biocathodes as efficient, robust, and alternatives to natural laccase, offering significant advantages for oxygen reduction catalysis and biofuel cell performance optimization.

The electrochemical characterization clearly demonstrates that nCuCeAuZIF provides the highest overall electrochemical performance, emphasizing the strong potential of LacNZs as efficient, durable, and scalabl cathodic materials suitable for enzymatic biofuel cells and related bioelectrocatalytic applications.

3.4. Oxygen Reduction Reaction on LacNZ-Based Cathodes

To evaluate the electrocatalytic activity of the synthesized laccase mimetics toward the oxygen reduction reaction (ORR), only-LacNZs-based electrodes (nCuCeAuZIF/GCE, nCoCuCeZIF/GCE, and nPtCu/GCE) were fabricated, and CV measurements were performed (Figure 4). The measurements were carried out in 0.05 M AB (pH 4.5), containing 1 mM ABTS under both argon- or air-saturated conditions at a scan rate of 25 $mV \cdot s^{-1}$.

Under argon-saturated conditions, all LacNZ-modified electrodes exhibited only weak, broad redox features, reflecting intrinsic redox transitions within the metallic centers and confirming the absence of oxygen-reduction processes. Upon air in cathodic current was observed within rang −0.5 to −0.7 V vs. Ag/AgCl (Figure 4), signifying activation of ORR. Although the CV profiles do not display well-defined cathodic peaks, the monotonic current increase is characteristic of ORR on heterogeneous NZ-based catalysts, where oxygen adsorption, electron transfer, and protonation steps occur concurrently. The level of current enhancement was strongly dependent on electrode composition. The nCuCeAuZIF/GCE cathode exhibited the highest ORR activity, reaching approximately −28 μA at −0.60 V vs. Ag/AgCl (Figure 4A). The nCoCuCeZIF/GCE electrode demonstrated a similar, though more moderate, response (≈−16 μA at −0.60 V) (Figure 4B), whereas the nPtCu/GCE cathode showed only a minor increase (≈−5 μA) (Figure 4C), indicating limited oxygen-reduction capability. In contrast to the text LacNZ-modified electrodes, the control electrode based on the native enzyme, Lac/GCE (Figure 4D), displayed distinct electrochemical behaviour in the presence of ABTS mediator. Specifically, Lac/GCE exhibited a clear, quasi-reversible redox peak pair centered at approximately +0.6 V vs. Ag/AgCl, highlighting the catalytic turnover of ABTS by laccase.

The high activity of the multimetallic LacNZs from synergistic electronic interactions among Au^0, Cu^+/Cu^{2+}, Ce^{3+}/Ce^{4+}, and Co^{2+}/Co^{3+} centers. Au^0 facilitates electron delocalization and improves charge transport**,** while the Ce^{3+}/Ce^{4+} redox pair supports reversible oxygen activation via formation of surface oxygen vacancies, whereas Co^{2+}/Co^{3+} primarily enhances proton-coupled electron transfer (PCET). Together, these redox-active sites, including the Cu centers, establish a cooperative multielectron transfer network that lowers the activation barrier for oxygen reduction and promotes efficient charge transport**.** This behavior closely parallels the functional organization of the T1–T3 copper cluster in natural laccase, providing a bioinspired multielectron pathway for ORR. Specifically, Cu^+/Cu^{2+} sites act as key electron donors during O_2 reduction, enhancing the adsorption of oxygen molecules on the catalyst surface and promoting rapid electron transfer through the multimetallic network. Ce^{3+}/Ce^{4+} cycling, in particular, facilitates quasi-four-electron ORR by stabilizing $O_2\bullet^-$ and HO_2^- intermediates, whereas the presence of Co^{2+}/Co^{3+} enhances proton-coupled electron transfer (PCET), which is essential for efficient ORR under acidic conditions. The structural confinement imposed by the ZIF framework further contributes to catalytic efficiency by stabilizing metal centers, preventing nanoparticle aggregation, and ensuring uniform dispersion of redox-active sites. Similar confinement effects have been widely associated with improved ORR onset potentials and increased diffusion-limited currents in metal–organic-framework-derived NZs.

Overall, the nCuCeAuZIF catalyst exhibited the highest ORR efficiency among the tested materials, enabling rapid and sustained oxygen activation through a cooperative electron-transfer mechanism that closely resembles natural laccase. The ability of this material to deliver stable cathodic currents without distinct peak formation reflects a kinetically controlled ORR regime typical of advanced heterogeneous electrocatalysts. These findings underscore the strong potential of LacNZ-based cathodes for enzymatic biofuel cell applications, where high ORR activity, operational stability, and efficient multielectron transfer are essential.

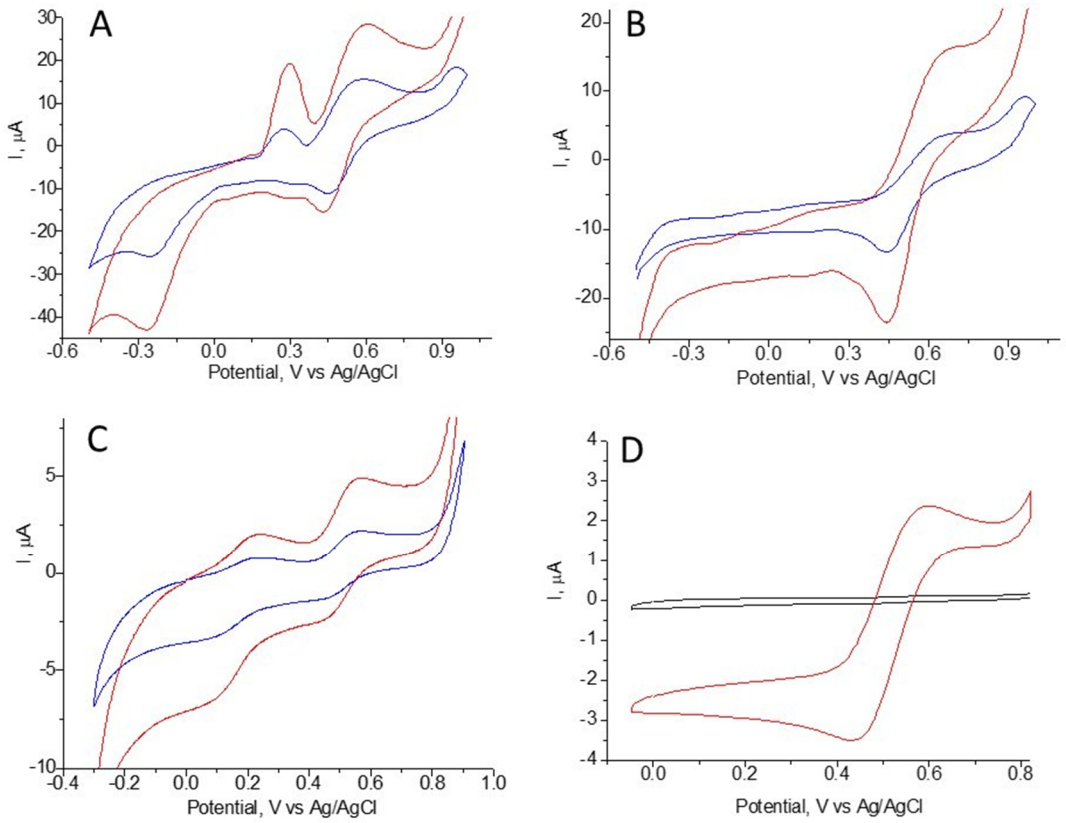

Figure 4. CV curves of (**A**) nCuCeAuZIF/GCE, (**B**) nCoCuCeZIF/GCE, (**C**) nPtCu/GCE and **(D)** Lac/GCE, cathodes recorded in argon (blue line) and air-saturated (red line) 0.05 M AB (pH 4.5), containing 1 mM ABTS at a scan rate of 25 mV·s^{-1}.

3.5. Electrochemical Performance of the Enzymatic Biofuel Cells

To evaluate the electrocatalytic activity and practical applicability of the synthesized LacNZs as cathodic catalysts, several enzyme-based fuel cells (EBFCs) were constructed employing different biocathode configurations. All EBFCs featured the same anodic architecture, based on alcohol oxidase (AOx) immobilized on CNT-modified glassy carbon electrodes (AOx/CNTs/GCE), and operated in 50 mM phosphate buffer (pH 7.5) with 1 mM hydroquinone (HQ) as the anodic redox mediator [14]. The tested cathodes consisted of: (i) natural laccase (Lac/GCE), (ii) hybrid Lac/LacNZ composites, and (iii) enzyme-free only LacNZ-based electrodes, enabling a direct comparison of enzymatic, hybrid and enzyme-free systems under identical experimental conditions. The schematic configuration of the constructed EBFCs is shown in Figure 5.

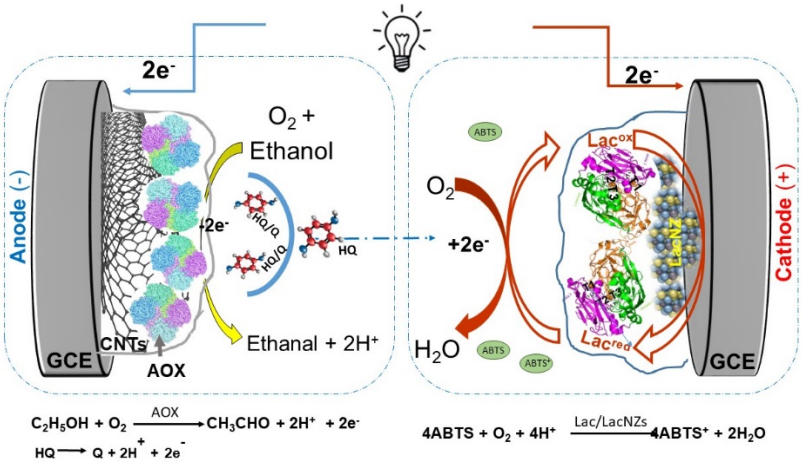

Figure 5. Schematic illustration of the developed enzymatic biofuel cell (EBFC) featuring an bioanode (AOx/CNT/GCE) and a hybrid cathode (Lac/LacNZs/GCE). The redox mediators: HQ at the anode and ABTS at the cathode.

The main electrochemical parameters, open-circuit potential (OCV), power density, short-circuit current (ISC), and current density, are summarized in Table 2. To evaluate the influence of catalytic cathode composition on overall EBFC performance, all systems were compared under identical experimental conditions. The reference EBFC with a natural laccase cathode exhibited OCV = 0.600 V**,** power density = 0.267 μW·cm^{-2}, ISC = 113 nA, and current density = 1.60 μA·cm^{-2} highlighting the baseline enzymatic activity (Figure 6 and Table 2). Integration of LacNZs into the cathodic layer markedly enhanced both power output and current density**,** demonstrating that the NZ framework effectively promotes interfacial electron transfer and accelerates oxygen reduction reaction (ORR) kinetics.

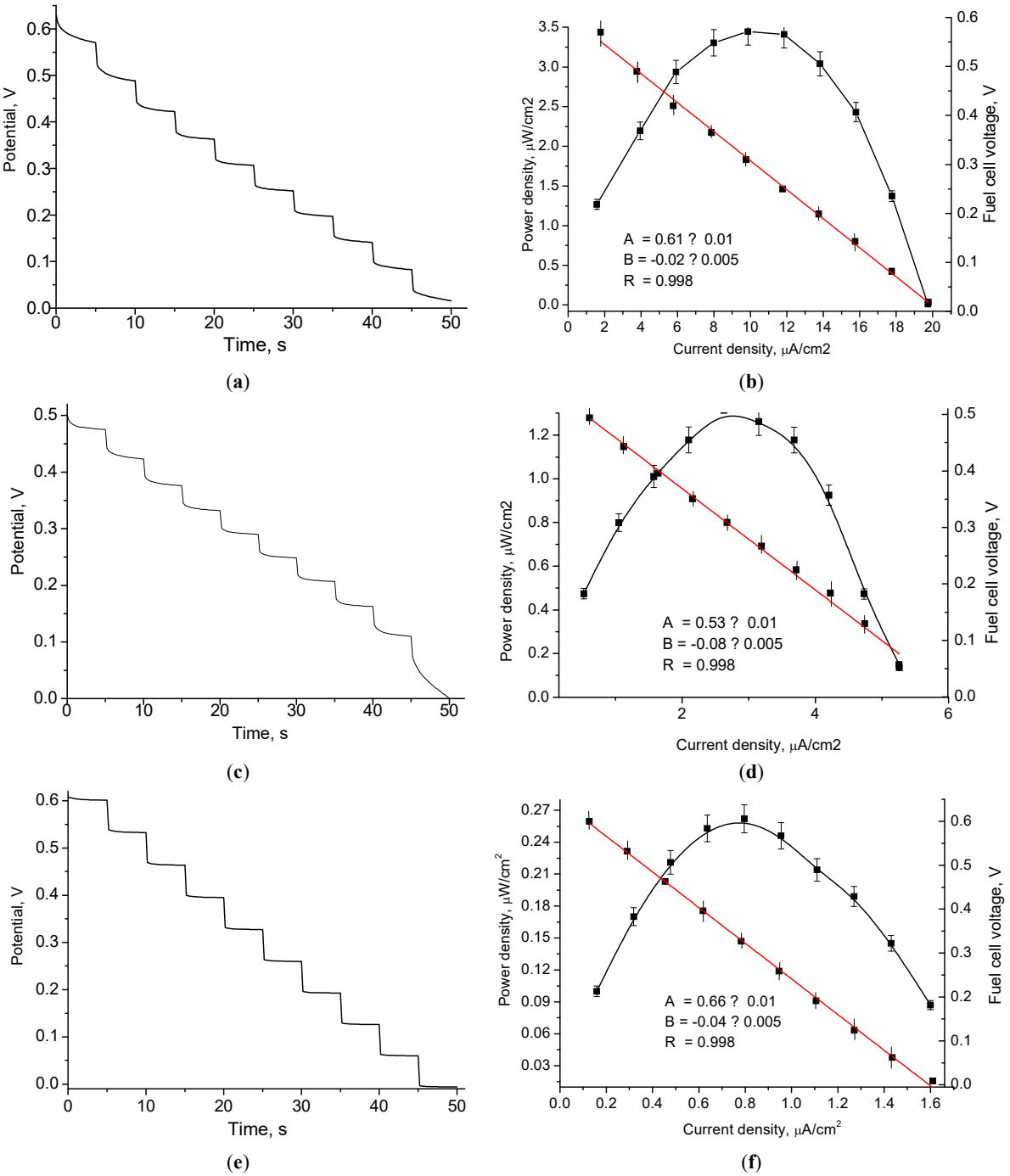

Figure 6. EBFC performance with different cathodes: (**a**,**b**) Lac/nCuCeAuZIF/GCE; (**c**,**d**) Lac/nCuCeZIF/GCE; (**e**,**f**) Lac/GCE. Time-dependent potential decay (**a**,**c**,**e**)—polarization (red) and power density (black) curves (**b**,**d**,**f**) in 1 mM ethanol (hydroquinone mediator for bioanode: AOx/CNTs/GCE) and 1 mM ABTS for cathode.

Among all tested configurations, the Lac/nCuCeAuZIF/GCE hybrid cathode demonstrated the highest performance, achieving OCV = 0.610 V**,** power density = 3.4 μW·cm^{-2}, ISC = 610 nA, and **c**urrent density = 12.5 μA·cm^{-2} (Figure 6). The Lac/nCoCuCeZIF/GCE electrode also demonstrated good electrochemical characteristics

(OCV = 0.550 V, power density = 1.2 μW·cm^{-2}, ISC = 660 nA, current density = 6.1 μA·cm^{-2}). In contrast, the Lac/nPtCu/GCE configuration produced the highest OCV (0.747 V), but a lower ISC and current density (111 nA, 2.1 μA·cm^{-2}), indicating slower electron transfer at the cathode. Enzyme-free nanozyme cathodes (nCuCeAuZIF/GCE and nCoCuCeZIF/GCE) retained significant intrinsic ORR activity (1.3 μW·cm^{-2}, 175 nA, 2.4 μA·cm^{-2} and 0.53 μW·cm^{-2}, 110 nA, 3.42 μA·cm^{-2}, respectively), confirming that LacNZs can act as independent cathodic catalysts (Table 2).

Table 2. Effect of cathodes composition on EBFC performance.

Bioanode	Biocathode	OCV (V)	Power Density (μW/cm^2)	Short-Circuit Current, (nA)	Current Density (μA/cm^2)
AOx/CNTs/GCE	Lac/GCE	0.600	0.267	113	1.60
AOx/CNTs/GCE	Lac/nCuZIF/GCE	0.519	0.510	282.17	2.20
AOx/CNTs/GCE	Lac/nCoZIF/GCE	0.334	0.409	360.00	2.83
AOx/CNTs/GCE	Lac/nPtCu/GCE	0.747	0.794	111.0	2.1
AOx/CNTs/GCE	Lac/nCoCuCeZIF/GCE	0.550	1.2	660	6.1
AOx/CNTs/GCE	Lac/nCuCeAuZIF/GCE	0.610	3.4	610	12.5
AOx/CNTs/GCE	nCuCeAuZIF/GCE	0.510	1.3	175	2.4
AOx/CNTs/GCE	nCoCuCeZIF/GCE	0.560	0.53	110	3.42

When compared with similar laccase-based cathodes reported in the literature (Table 3), the current hybrid systems (Lac–LacNZ) demonstrate a marked improvement in overall performance. Conventional configurations such as Lac/GCE (0.267 μW·cm^{-2}, OCV = 0.60 V) and GC/MWCNTs/PTb/Ppy (2.3 μW·cm^{-2}, OCV = 0.37 V) show substantially lower OCV [15]. In contrast, green-synthesized Lac/AgNP/PGE-2B and Lac/CuNP/PGE-2B cathodes yielded 20.6 μW·cm^{-2} and 17.4 μW·cm^{-2}, respectively, though these were obtained under different anodic configurations, limiting direct comparability. Notably, the Lac/nCuCeAuZIF/GCE system exhibited a ~16-fold increase in power density relative to Lac/GCE, highlighting the strong synergistic effect of LacNZs. The hybrid cathodes also show excellent reproducibility, with replicate EBFCs demonstrating <5% variation in power output. The performance also surpasses previously reported AOx/nAgCu/GCE (1.30 μW·cm^{-2}) and AOx/nAgCePt/GCE (1.04 μW·cm^{-2}) configurations [14]. Although some literature examples achieve higher current densities (e.g., AlO/CNNT/PANi/Lac:140.2 μA·cm^{-2}, OCV = 0.59 V) [16], PGE/PANi/MWCNT/Lac:1209 μA·cm^{-2}, OCV = 0.528 V [17] and NA-MWCNT/Lac/GCE: 3300 μA·cm^{-2}) [18], the present Lac/nCuCeAuZIF/GCE configuration provides one of the most favorable OCV-current density balances, placing it among the most efficient LacNZ-based cathodes constructed on the AOx/CNTs platform.

Table 3. Characteristics of EBFCs described in the literature.

Bioanode	Biocathode	OCV, V	Power Density (μW/cm^2)	Current Density (μA/cm^2)	Short-Circuit Current, (ISC, nA)	Refs.
AOx/GCE	Lac/GCE	0.58	0.20	-	100	[14]
AOx/nAgCu/GCE	Lac/nAuCePt	0.54	1.30	-	700	[14]
AOx/nAgCePt/GCE	Lac/nAuCePt	0.50	1.04		600	[14]
CNT/PBA/HRP/PEI/GOx	-	0.31	-	38.7	-	[19]
GR/PB-PPCA/PPCA-GOx	-	0.490	-	85.86	-	[20]
-	CNT/PEI/GNP/NTP/Lac	0.70	13	93	-	[21]
-	CNT/PEI/GNP/Lac	0.30	4	49	-	[21]
-	Lac/AP-tGO/GCE	0.526	-	151.4		[22]
-	NA-MWCNT/Lac/GCE	0.50	-	3300	-	[18]
-	Nafion/MWCNT/Tyro	0.30	-	550	-	[23]
-	GC/MWCNTs/PTb/Ppy	0.37	2.3	31.7	-	[24]
-	CNBP/Lac	0.557	-	50	-	[25]
-	MWCNT/Lac	0.430	160	1209.2	-	[26,16]
-	AlO/CNNT/PANi/Lac	0.59	-	140.2	-	[16]

Table 3. *Cont.*

Bioanode	Biocathode	OCV, V	Power Density (μW/cm^2)	Current Density (μA/cm^2)	Short-Circuit Current, (ISC, nA)	Refs.
-	PGE/PANi/MWCNT/Lac	0.528	-	1209	-	[17]
Pt rod	PG/PA/MWCNT/Lac	0.60	-	295.7	-	[27,28]
Pt rod	Lac/CuNP/PGE-2B	0.498	17.39	1054.17	-	[1]
Pt rod	Lac/AgNP/PGE-2B	0.611	20.629	1343.15	-	[1]

Abbreviation: AlO—Al_2O_3; AP-tGO-Amino-functionalized tGO; CNT—carbon nanotubes; CNNT—Carbon Nanotubes; CNBP—cellular nucleic acid–binding protein; MWCNT—multi-walled carbon nanotubes; NA-MWCNT-Nitrogen-doped MWCNT; GNP—gold nanoparticles; GOx—glucose oxidase; HRP—horseradish peroxidase; Lac—laccase; Tyro—tyrosinase; PBA—prussian blue analogue; PEI—polyethyleneimine; PTb—prussian blue–tetrabenzoporphyrin composite, Ppy—polypyrrole; PPCA—Polymer; PB-PPCA-Prussian Blue-Polymer Composite; GCE—glassy carbon electrode; GE—graphene electrode; GO—graphene oxide; tGO—thiolated graphene oxide; PGE—pencil graphite electrode; PGE-2B—pencil graphite electrode hardness grade 2B; PANi—polyaniline; NP—nanoparticle.

The observed improvements arise from a bioinorganic redox synergy, wherein LacNZs contain multiple redox-active sites (Co^{2+}/Co^{3+}, Cu^{+}/Cu^{2+}, Ce^{3+}/Ce^{4+}, Au^{0}/Au^{+}) that mimic the multicopper cluster of natural laccase. The cooperative redox interactions between the T_1–T_3 centers of laccase and the metallic sites of the NZ facilitate rapid electron transfer, enable direct four-electron O_2 reduction to H_2O, and stabilize the enzyme's electroactive conformation, leading to enhanced durability (Figure 7).

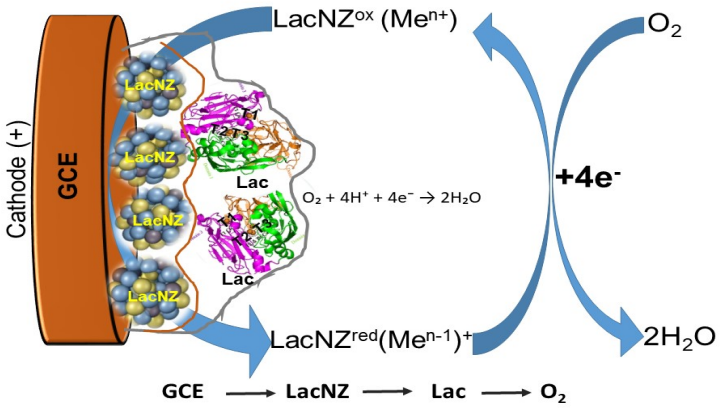

Figure 7. Schematic illustration of the synergistic electrocatalytic mechanism for the hybrid cathode nCuCeAuZIF/Lac/GCE. LacNZ—laccase-like nanozyme, Lac-laccase *T. zonata.*

Importantly, the only-LacNZs-based cathodes (enzyme-free)—nCuCeAuZIF-NZ/GCE and nCoCuCeZIF-NZ/GCE—retained substantial intrinsic ORR activity, with power densities of 1.2 and 0.546 μW·cm^{-2}, respectively. This constitutes the first experimental evidence that LacNZs can act as independent cathodic catalysts, offering a promising route toward EBFCs with improved durability and reduced cost. However, their performance remains lower than hybrid electrodes (Lac/LacNZ), emphasizing the synergistic interplay between enzymatic and NZ components. Laccase provides substrate specificity and multicopper redox centers, whereas the NZ matrix enhances electron mobility, active-site density, and interfacial stability. The integration of these effects results in higher current densities, lower internal resistance, and superior energy conversion efficiency.

Chronoamperometric stability tests demonstrated that nCuCeAuZIF-NZ/GCE and nCoCuCeZIF-NZ/GCE retained 90–92% of initial activity after 20 h of continuous operation, outperforming typical enzyme-based cathodes, which lose >50% activity within 5 h. These results confirm the enhanced operational stability and reproducibility of LacNZ-integrated cathodes.) Section 3.5. Electrochemical performance of the enzymatic biofuel cells.

Overall, the integration of natural laccase with multimetallic LacNZs produces a robust and efficient cathodic platform that bridges enzymatic selectivity with enhanced electron transport, stability, and high current density. The ability of LacNZs to function independently highlights a promising direction for future EBFC design, enabling durable, high-performance, and environmentally benign electrochemical energy technologies.

3.6. Stability of Lac/nCuCeAuZIF/GCE and Comparison with Laccase-Only Cathodes

The storage stability of the Lac/nCuCeAuZIF/GCE hybrid cathode was systematically evaluated and directly compared with only laccase-base (Lac/GCE) electrode. Relative current responses of both electrodes were monitored over 14 days at storage 4 °C and as using the substrate 0.1 mM ABTS at an applied potential of −0.1 V. The hybrid biocathode retained 75% of its initial current response after 10 days, whereas the only laccase-base electrode preserved only 30% under the same conditions. This result confirms the stabilizing function of the nCuCeAuZIF NZ toward native laccase (Figure 8A).

The effect of temperature on the electrocatalytic performance was also examined for both electrodes. The hybrid electrode showed maximal activity at 25–30 °C range. while operation above 30 °C resulted in a progressive decrease in current, consistent with thermal inactivation of laccase (Figure 8B). The temperature profile of the hybrid electrode closely followed that of free laccase, indicating that the NZ improves stability without altering the intrinsic thermal optimum of natural laccase.

Similarly, pH-dependent studies demonstrated that both electrodes showed the highest catalytic currents at pH 4.5, while currents decreased substantially at pH > 6.0 (Figure 8C), in agreement with the acidic optimum of laccase and the catalytic characteristics of the NZ. These results show that the incorporation of nCuCeAuZIF enhances long-term stability while preserving the inherent pH and temperature optima of the enzyme. Improved durability is attributed to (i) structural and electrostatic protection of the enzyme by the NZ matrix, and (ii) the auxiliary contribution of the NZ to ORR, which lowers the catalytic load on laccase.

Importantly, the hybrid electrode also demonstrated exceptional resistance to high ionic strength—an essential parameter for operation in complex biological fluids. When exposed to 0.25 M NaCl, the sensitivity of the laccase-only Lac/GCE electrode decreased markedly from 1.2 to 0.7 μA·mM^{-1} (−41.7%). In contrast, the Lac/nCuCeAuZIF/GCE electrode not only maintained its performance but exhibited a slight increase in sensitivity, from 4.0 to 4.3 μA·mM^{-1} (+7.5%) (Figure 8D). This result highlights the protective role of the nCuCeAuZIF NZ, which provides a stabilizing microenvironment that the immobilized enzyme from ionic-strength-induced destabilization and preserves efficient electron transfer under physiologically relevant conditions.

The repeatability of the Lac/nCuCeAuZIF/GCE biocathode was assessed by performing five successive amperometric measurements with a single Lac/nCuCeAuZIF/GCE electrode in the presence of ABTS. The current responses exhibited a low relative standard deviation (RSD) of 2.6% (Figure 8F), indicating high signal consistency and minimal drift during repeated operation.

To evaluate the reproducibility of the electrode fabrication procedure, five independently prepared Lac/nCuCeAuZIF/GCE electrodes were tested under identical electrochemical conditions. When aded to 0.1 mM ABTS, the variation in oxidation current yielded an RSD of 3.6% ((Figure 8E). This low value confirms high batch-to-batch consistency, reflecting both the reliability of the fabrication procedure and the uniform catalytic performance of the nCuCeAuZIF coating.

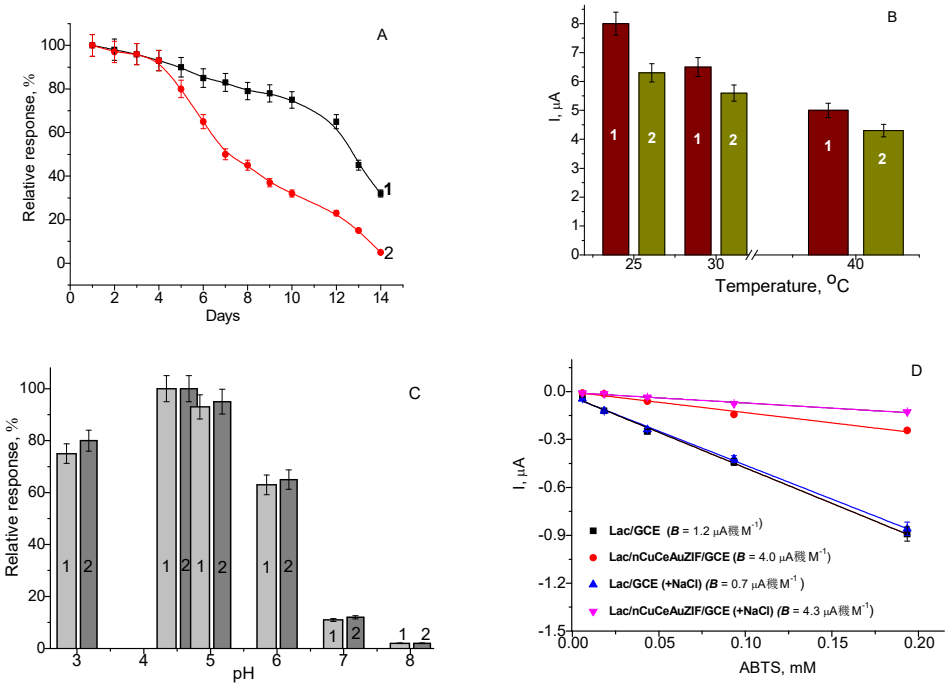

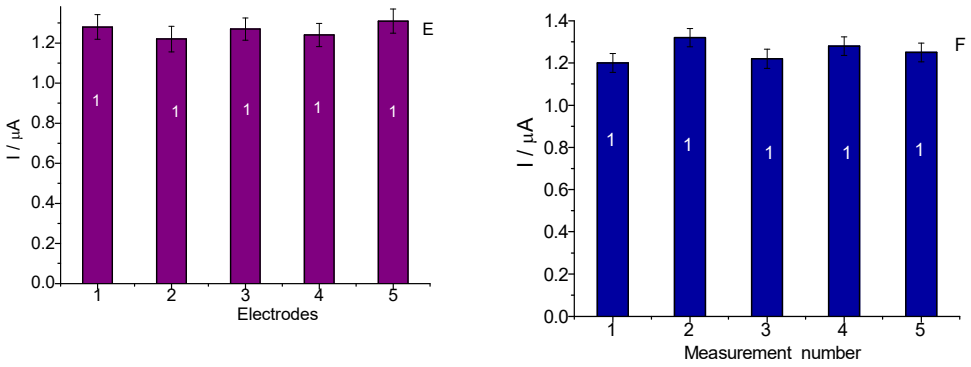

Figure 8. Stability, environmental tolerance, and analytical reliability of the Lac/nCuCeAuZIF/GCE (**1**) and Lac/GCE (**2**) biocathodes. (**A**) Storage stability; (**B**) Temperature dependence; (**C**) pH dependence (using 0.05 M phosphate buffer (pH 6.0, 7.0, 8.0) and 0.05 M acetate buffer (pH 3.0, 4.5, 5.0)); (**D**) Ionic strength tolerance (Sensitivity values (B, $\mu A \cdot mM^{-1}$); (**E**) Reproducibility; (**F**) Repeatability.

4. Conclusions

This study presents a significant advancement in the development of high-performance cathodes for enzymatic biofuel cells (EBFCs) through the rational design of hybrid cathodes laccase/laccase-like nanozyme (Lac/LacNZs). Laccase from *Trametes zonata* was integrated with a series of LacNZs, including nCoZIF, nCuZIF, nPtCu, nCoCuCeZIF, and nCuCeAuZIF, to construct bioinorganic cathodes with enhanced oxygen reduction reaction (ORR) activity, Among them, the Lac/nCuCeAuZIF/GCE and Lac/nCoCuCeZIF/GCE cathodes achieving power densities of 3.4 $\mu W \cdot cm^{-2}$ (OCV = 0.610 V) and 2.2 $\mu W \cdot cm^{-2}$ (OCV = 0.550 V), respectively. These values represent a substantial improvement over the laccase-based cathode (Lac/GCE), which produced 0.267 $\mu W \cdot cm^{-2}$ (OCV = 0.600 V), confirming the strong performance enhancement provided by LacNZ incorporation. The achieved performance is attributed to a synergistic redox coupling between the multicopper centers of the natural enzyme and the redox-active metallic elements NZs (Co^{2+}/Co^{3+}, Cu^{+}/Cu^{2+}, Ce^{3+}/Ce^{4+}) within the cathodic layer. This interaction enhances electron transfer efficiency, enables a direct four-electron oxygen reduction pathway, and results in reduced resistance and improved stability. Importantly, this study provides the first experimental evidence that LacNZs can function as independent cathodic catalysts, maintaining substantial ORR activity in the absence of laccase and achieved power densities of 1.2 $\mu W \cdot cm^{-2}$ (nCuCeAuZIF/GCE) and 0.53 $\mu W \cdot cm^{-2}$ (nCoCuCeZIF/GCE) even in the absence of laccase. These results identify LacNZs as promising enzyme-free, reliable, and cost-effective nanomaterials with superior catalytic activity and stability. The hybrid Lac/nCuCeAuZIF/GCE cathode also demonstrated outstanding stability across multiple parameters: it retained 75% of its initial activity after 10 days at 4 °C, whereas the laccase-only electrode retained only 30%. The incorporation of LacNZs preserved the pH optimum 4.5 and temperature optimum (25 °C) of laccase, while significantly enhancing envirolmentas tolerance. Under high ionic strength (0.25 M NaCl), the hybrid cathode exhibited a 7.5% increase in sensitivity, in contrast to a 41.7% loss for the laccase-only electrode, highlighting the protective and stabilizing role of the NZ. Furthermore, goode repeatability (RSD = 2.6%) and reproducibility (RSD = 3.6%), validating the robustness of the fabrication.

Overall, this work provides the first experimental evidence that integrating natural laccase with its artificial mimetics yields a highly efficient, stable, and scalable bioinorganic biocathode platform. The developed LacNZ-based hybrid electrodes bridge the gap between biocatalytic selectivity and inorganic durability, establishing a strong foundation for next-generation EBFCs with enhanced power density and long-term performance. These findings underscore the transformative potential of LacNZ architectures as versatile, bioinspired cathodic materials for sustainable and high-efficiency bioelectrochemical energy systems.

Author Contributions

Conceptualization: O.D. and M.G.; methodology: O.D. and N.S.; software N.S. investigation: O.D. and N.S.; resources: M.G.; data curation: H.K., O.Z. and G.G.; writing—original draft preparation: O.D.; writing—review and editing: G.G., M.G. and N.S.; supervision: M.G.; project administration: G.G.; funding acquisition: M.G. All authors have read and agreed to the published version of the manuscript.

Funding

This research was supported by the NAS and ONRG (USA) in the frame of the program IMPRESS-U (project STCU 7113), the NAS of Ukraine (Reg. number 0125U001032), as well as by a Presidential Discretionary-Ukraine Support Grants" SFI-PD-Ukraine-00014576 from Simons Foundation, the Ministry of Education and Science of Ukraine, Grants 0125U001054, 0125U002005, and 0125U002033.

Data Availability Statement

Data is contained within the article.

Conflicts of Interest

The authors declare no conflict of interest. Given the role as the Editorial Board Member, Mykhailo Gonchar had no involvement in the peer review of this paper and had no access to information regarding its peer-review process. Full responsibility for the editorial process of this paper was delegated to another editor of the journal.

Use of AI and AI-Assisted Technologies

During the preparation of this work, the authors Olha Demkiv, Nataliya Stasyuk, Oksana Zakalska, Halyna Klepach, Galina Gayda and Mykhailo Gonchar used ChatGPT 4.0 in order to improve language of the paper. After using this service, the authors reviewed and edited the content and take full responsibility for the content of the publication

References

1. Keerthi, D.S.; Vani, M.M.; Likith, G.; et al. Nature-powered bio-cathodes: Synergistic effects of laccase immobilization and green nanoparticles on enhanced PGEs for sustainable biofuel cells. *Bioelectrochemistry* **2025**, *165*, 108996. https://doi.org/10.1016/j.bioelechem.2025.108996.
2. Nasar, A.; Perveen, R. Applications of enzymatic biofuel cells in bioelectronic devices—A review. *Int. J. Hydrogen Energy* **2019**, *44*, 15287–15312. https://doi.org/10.1016/j.ijhydene.2019.04.182.
3. Le Goff, A.; Holzinger, M.; Cosnier, S. Recent progress in oxygen-reducing laccase biocathodes for enzymatic biofuel cells. *Cell. Mol. Life Sci.* **2015**, *72*, 941–952. https://doi.org/10.1007/s00018-014-1828-4.
4. Fredj, Z.; Rong, G.; Sawan, M. Recent advances in enzymatic biofuel cells to power up wearable and implantable biosensors. *Biosensors* **2025**, *15*, 218. https://doi.org/10.3390/bios15040218.
5. Ghosh, B.; Saha, R.; Bhattacharya, D.; et al. Laccase and its source of sustainability in an enzymatic biofuel cell. *Bioresour. Technol. Rep.* **2019**, *6*, 268–278. https://doi.org/10.1016/j.biteb.2019.03.013.
6. Abdi Dezfouli, R.; Esmaeilidezfouli, E. Optimizing laccase selection for enhanced outcomes: A comprehensive review. *3 Biotech* **2024**, *14*, 165. https://doi.org/10.1007/s13205-024-04015-5.
7. Horiguchi, H.K.; Semba, H.; Yamada, H.; et al. Bilirubin oxidase expression and activity enhancement from *Myrothecium verrucaria* in *Aspergillus* species. *J. Biosci. Bioeng.* **2024**, *138*, 212–217. https://doi.org/10.1016/j.jbiosc.2024.06.002.
8. Demkiv, O.; Nogala, W.; Stasyuk, N.; et al. Laccase mimetics as sensing elements for amperometric assay of 5-hydroxyindoleacetic acid in urine. *Bioelectrochemistry* **2025**, *161*, 108839. https://doi.org/10.1016/j.bioelechem.2024.108839.
9. Alizadeh, N.; Ghasemi, S.; Salimi, A.; et al. CuO nanorods as a laccase-mimicking enzyme for highly sensitive colorimetric and electrochemical dual biosensor: Application in living cell epinephrine analysis. *Colloids Surf. B Biointerfaces* **2020**, *195*, 111228. https://doi.org/10.1016/j.colsurfb.2020.111228.
10. Vetr, F. Colorimetric detection platforms based on enzyme-mimetic activities of metal (M)-substituted vanadates (MxVyOz): A review of synthesis, mechanisms, and sensing applications. *Microchem. J.* **2025**, *218*, 115271. https://doi.org/10.1016/j.microc.2025.115271.
11. Tian, C.; Maheu, C.; Huang, X.; et al. Evaluating the electronic structure and stability of epitaxially grown Sr-doped $LaFeO_3$ perovskite alkaline O_2 evolution model electrocatalysts. *RSC Appl. Interfaces* **2025**, *2*, 122. https://doi.org/10.1039/D4LF00260A.
12. Demkiv, O.; Stasyuk, N.; Gayda, G.; et al. Highly sensitive amperometric sensor based on laccase-mimicking metal-based hybrid nanozymes for adrenaline analysis in pharmaceuticals. *Catalysts* **2021**, *11*, 1510. https://doi.org/10.3390/catal11121510.
13. Demkiv, O.; Nogala, W.; Stasyuk, N.; et al. Highly sensitive amperometric sensors based on laccase-mimetic nanozymes for the detection of dopamine. *RSC Adv.* **2024**, *14*, 5472–5478. https://doi.org/10.1039/D3RA07587G.
14. Demkiv, O.; Stasyuk, N.; Gayda, G.; et al. Biofuel cells based on oxidoreductases and electroactive nanomaterials: Development and characterization. *Biosensors* **2025**, *15*, 249. https://doi.org/10.3390/bios15040249.

15. Zebda, A.; Gondran, C.; Le Goff, A.; et al. Mediatorless high-power glucose biofuel cells based on compressed carbon nanotube–enzyme electrodes. *Nat. Commun.* **2011**, *2*, 1365. https://doi.org/10.1038/ncomms1365.
16. Kashyap, D.; Yadav, R.S.; Gohil, S.; et al. Fabrication of vertically aligned copper nanotubes as a novel electrode for enzymatic biofuel cells. *Electrochim. Acta* **2015**, *167*, 213–218. https://doi.org/10.1016/j.electacta.2015.03.164.
17. Bandapati, M.; Dwivedi, P.K.; Krishnamurthy, B.; et al. Screening various pencil leads coated with MWCNT and PANI as enzymatic biofuel cell biocathode. *Int. J. Hydrogen Energy* **2017**, *42*, 27220–27229. https://doi.org/10.1016/j.ijhydene.2017.09.016.
18. Ben Tahar, A.; Ramezanpour, M.; Reuillard, B.; et al. High catalytic performance of laccase wired to naphthylated multiwall carbon nanotubes. *Biosens. Bioelectron.* **2020**, *151*, 111961. https://doi.org/10.1016/j.bios.2019.111961.
19. Christwardana, M.; Kim, D.H.; Chung, Y.; et al. A hybrid biocatalyst consisting of silver nanoparticle and naphthalenethiol self-assembled monolayer prepared for anchoring glucose oxidase and its use for an enzymatic biofuel cell. *Appl. Surf. Sci.* **2018**, *429*, 180–186. https://doi.org/10.1016/j.apsusc.2017.07.023.
20. Kausaite-Minkstimiene, A.; Kaminskas, A.; Ramanaviciene, A. Development of a membraneless single-enzyme biofuel cell powered by glucose. *Biosens. Bioelectron.* **2022**, *216*, 114657. https://doi.org/10.1016/j.bios.2022.114657.
21. Kang, S.; Yoo, K.S.; Chung, Y.; et al. Cathodic biocatalyst consisting of laccase and gold nanoparticle for improving oxygen reduction reaction rate and enzymatic biofuel cell performance. *J. Ind. Eng. Chem.* **2018**, *62*, 329–332. https://doi.org/10.1016/j.jiec.2018.01.011.
22. Zhou, X.H.; Huang, X.R.; Liu, L.H.; et al. Direct electron transfer reaction of laccase on a glassy carbon electrode modified with 1-aminopyrene functionalized reduced graphene oxide. *RSC Adv.* **2013**, *3*, 18036–18043. https://doi.org/10.1039/c3ra42312c.
23. Reuillard, B.; Le Goff, A.; Agnès, C.; et al. Direct electron transfer between tyrosinase and multi-walled carbon nanotubes for bioelectrocatalytic oxygen reduction. *Electrochem. Commun.* **2012**, *20*, 19–22. https://doi.org/10.1016/j.elecom.2012.03.045.
24. Ammam, M.; Fransaer, J. Combination of laccase and catalase in construction of H_2O_2–O_2 based biocathode for applications in glucose biofuel cells. *Biosens. Bioelectron.* **2013**, *39*, 274–281. https://doi.org/10.1016/j.bios.2012.07.066.
25. Kipf, E.; Sané, S.; Morse, D.; et al. An air-breathing enzymatic cathode with extended lifetime by continuous laccase supply. *Bioresour. Technol.* **2018**, *264*, 306–310. https://doi.org/10.1016/j.biortech.2018.04.086.
26. Reuillard, B.; Dron, A.; Le Goff, A.; et al. One-year stability for a glucose/oxygen biofuel cell combined with pH reactivation of the laccase/carbon nanotube biocathode. *Bioelectrochemistry* **2015**, *106*, 73–76. https://doi.org/10.1016/j.bioelechem.2015.04.009.
27. Kashyap, D.; Yadav, R.S.; Gohil, S.; et al. Multi-walled carbon nanotube and polyaniline coated pencil graphite based bio-cathode for enzymatic biofuel cell. *Int. J. Hydrogen Energy* **2015**, *40*, 9515–9522. https://doi.org/10.1016/j.ijhydene.2015.05.120.
28. Dey, B.; Dutta, T. Laccases: Thriving the domain of bio-electrocatalysis. *Bioelectrochemistry* **2022**, *146*, 108144. https://doi.org/10.1016/j.bioelechem.2022.108144.